Supplementary material

Structural insights into alcohol dehydrogenases catalyzing asymmetric reductions

Jianhong An [1,4,5], Yao Nie [1,3]*, Yan Xu [1,2,3]*

[1] School of Biotechnology and Key Laboratory of Industrial Biotechnology, Ministry of Education, Jiangnan University, 1800 Lihu Road, Wuxi 214122, China
[2] State Key Laboratory of Food Science and Technology, Jiangnan University, 1800 Lihu Road, Wuxi 214122, China
[3] International Joint Research Laboratory for Brewing Microbiology and Applied Enzymology at Jiangnan University, 1800 Lihu Road, Wuxi 214122, China
[4] School of Ophthalmology and Optometry, Eye Hospital, Wenzhou Medical University, 270 Xueyuan Road, Wenzhou 325000, China
[5] State Key Laboratory of Optometry, Ophthalmology and Vision Science, 270 Xueyuan Road, Wenzhou 325000, China

*Address for correspondence:
Yao Nie and Yan Xu, School of Biotechnology and Key laboratory of Industrial Biotechnology, Ministry of Education, Jiangnan University, 1800 Lihu Road, Wuxi 214122, China.
Tel: +86-510-85197760. Fax: +86-510-85918201.
E-mail: ynie@jiangnan.edu.cn (Y. Nie); yxu@jiangnan.edu.cn (Y. Xu).

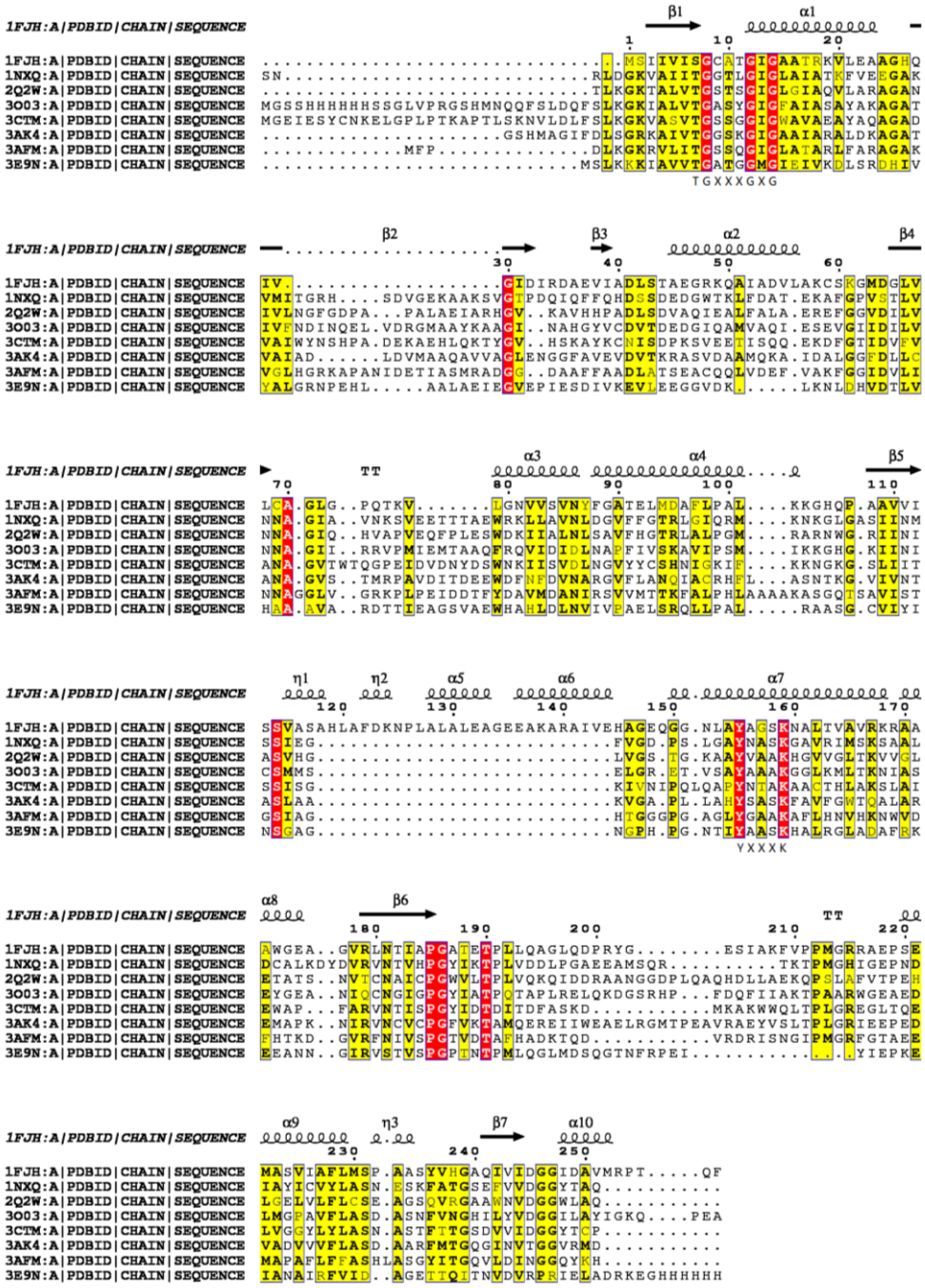

Supplementary Figure 1. Amino acid sequence alignment of various SDRs. Amino acid full-length sequences of SDRs (PDB IDs :1FJH; 1NXQ; 2Q2W; 3AFM; 3AK4; 3CTM; 3E9N; 3O03; 3PQD) were aligned using MAFFT online service (1). ESPript V3 (http://espript.ibcp.fr) was used to shade residues red or yellow that indicated the conserved amino acids (2). Numbering corresponds to 1FJH. Secondary structure elements of the 1FJH crystal structure are displayed. The NADP(H) binding motif (Thr-Gly-X-X-X-Gly-X-Gly) and an active site position (Tyr-X-X-X-Lys) are shown in the figure.

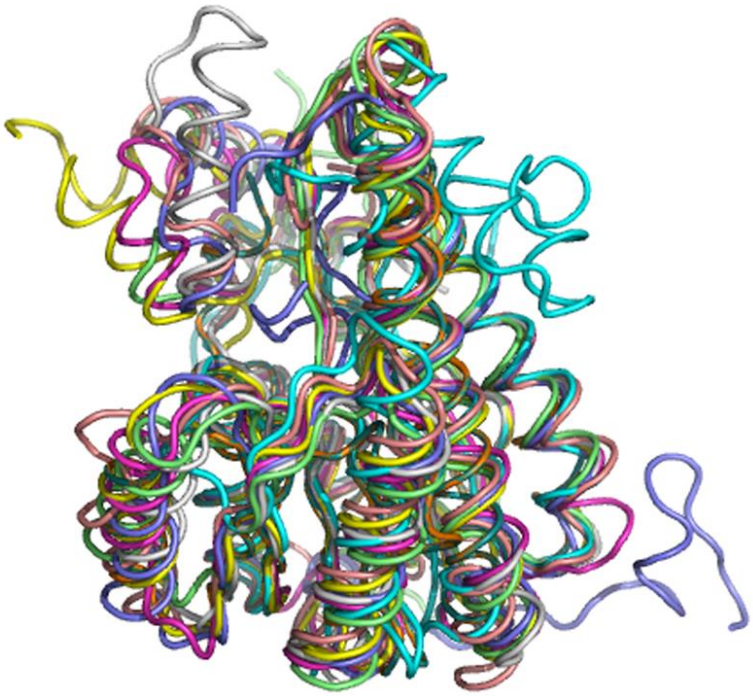

Supplementary Figure 2. Structural alignment of various SDRs. The backbone structures are shown in different colors with the PDB IDs (1FJH: cyan; 1NXQ: purple; 2Q2W: yellow; 3AFM: salmon; 3AK4: gray; 3CTM: slate; 3E9N: orange; 3O03: green; 3PQD: forest). Protein structures were retrieved from the RCSB PDB. PyMOL was used for 3D structural analysis and visualization.

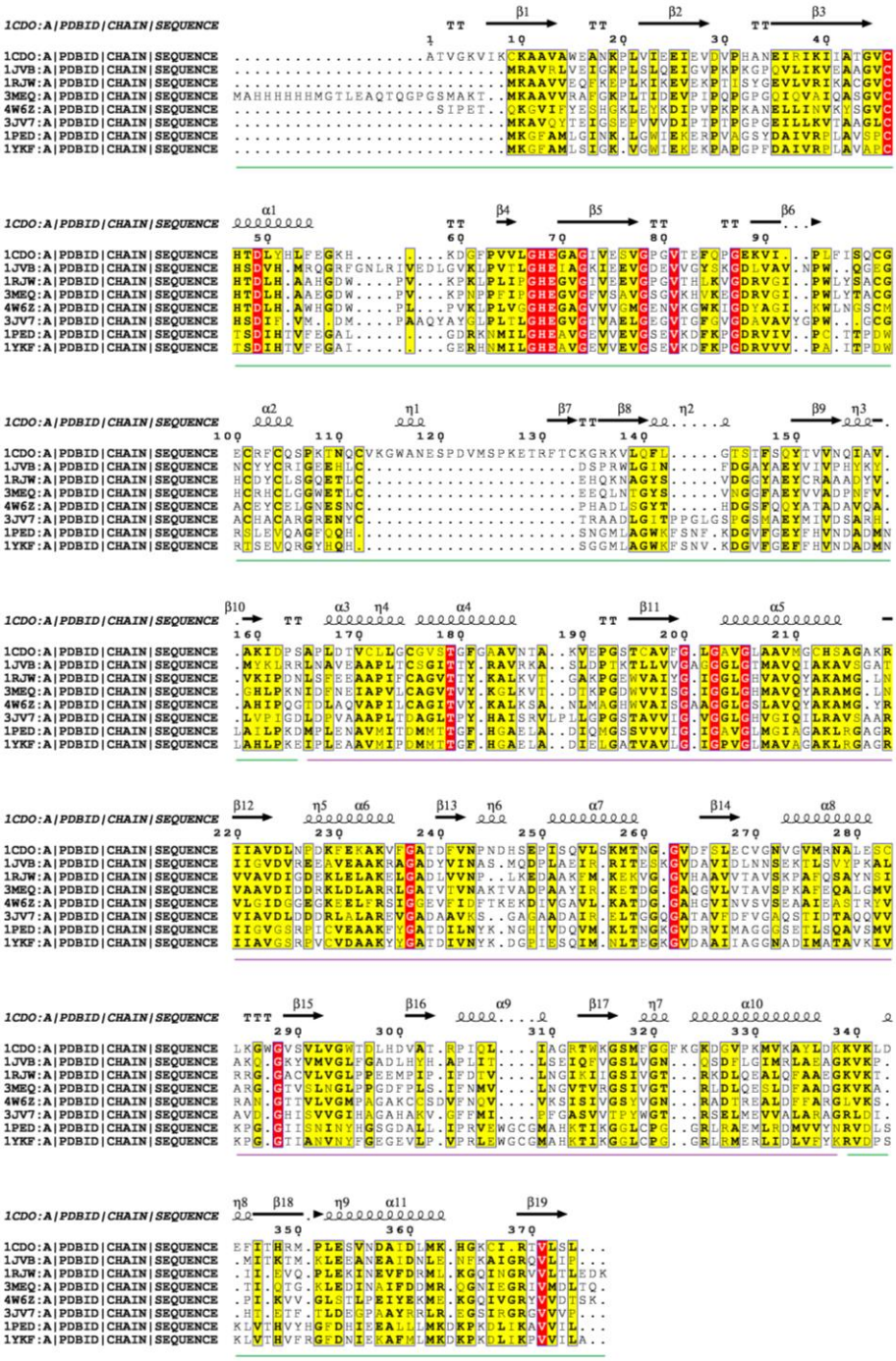

Supplementary Figure 3. Amino acid sequence alignment of various MDRs. Amino acid full-length sequences of MDRs (PDB IDs : 1CDO; 1JVB; 1PED; 1RJW; 1YKF; 4W6Z; 3JV7; 3MEQ) were aligned using MAFFT online service (1). ESPript V3 (http://espript.ibcp.fr) was used to edit residues (2). Numbering corresponds to 1CDO. Identical and similar amino acids are highlighted in red and yellow, respectively. Secondary structure elements of the 1CDO crystal structure are displayed. The substrate-binding domain and the cofactor-binding domain are indicated by green and purple bars, respectively.

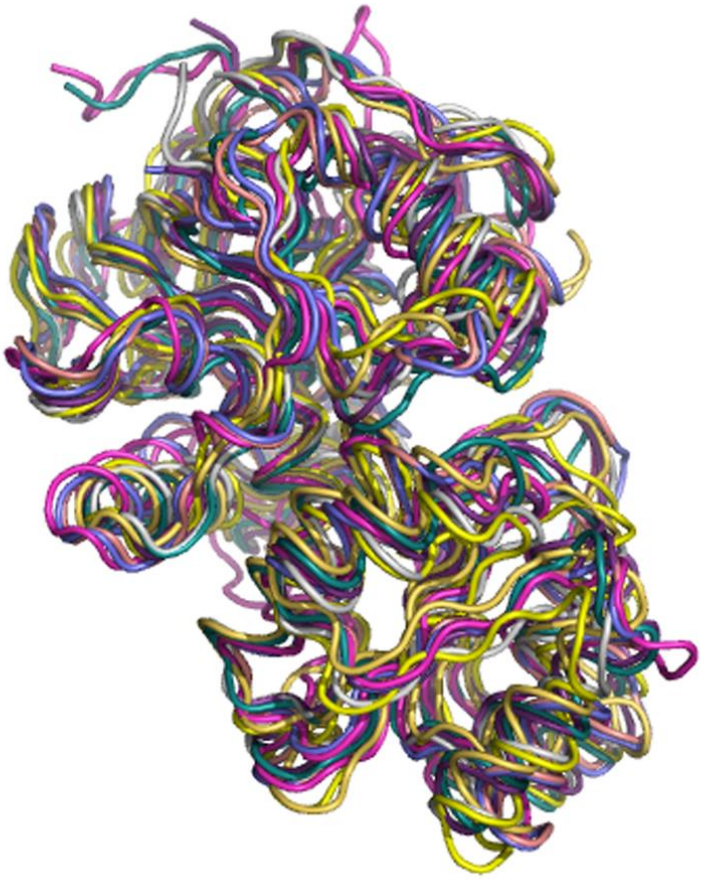

Supplementary Figure 4. Structural alignment of various MDRs. The backbone structures are shown in different colors with the PDB IDs (1CDO; 1JVB; 1PED; 1RJW; 1YKF; 4W6Z; 3JV7; 3MEQ). Protein structures were retrieved from the RCSB PDB. PyMOL was used for 3D structural analysis and visualization.

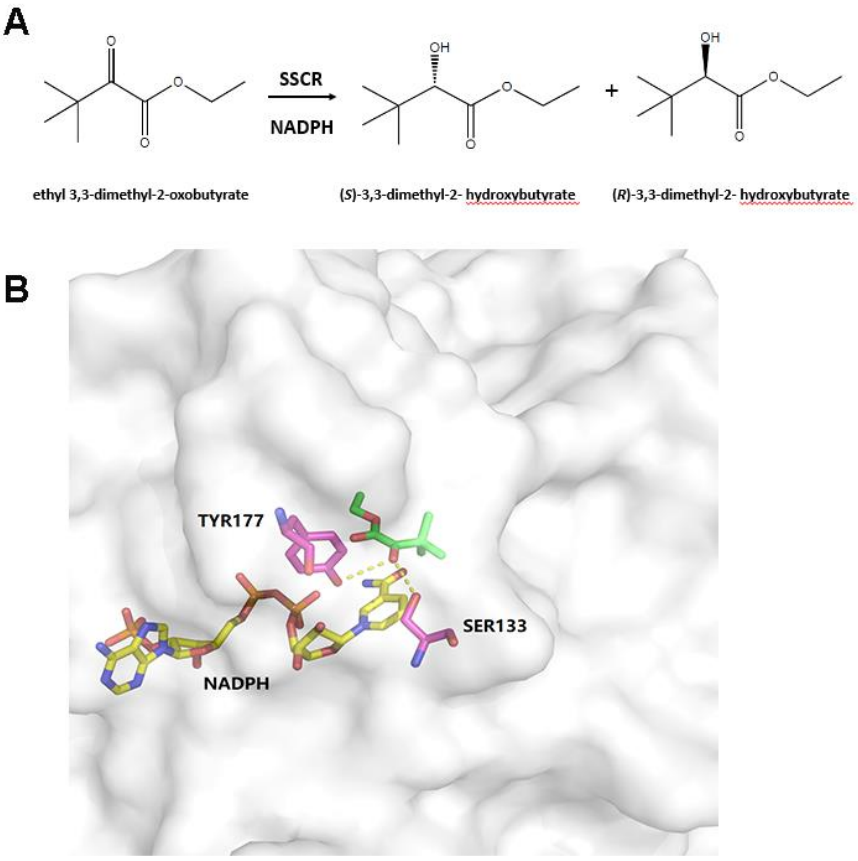

Supplementary Figure 5. (A) Reduction of ethyl 3,3-dimethyl-2-oxobutyrate by the carbonyl reductase from *Sporobolomyces salmonicolor* (SSCR). (B) Functional sites involved in the formation of substrate-binding pocket of SSCR (PDB ID: 1Y1P) with the ligands including ethyl 3,3-dimethyl-2-oxobutyrate and the cofactor NADH. The carbonyl oxygen atom of a substrate forms hydrogen bonds with both Tyr177 and Ser133 residues, and it is protonated from the Tyr177 residue, followed by the attacking of a hydride from C4 atom of NADPH to the carbonyl carbon atom of the substrate. PyMOL was used for 3D structural analysis and visualization.

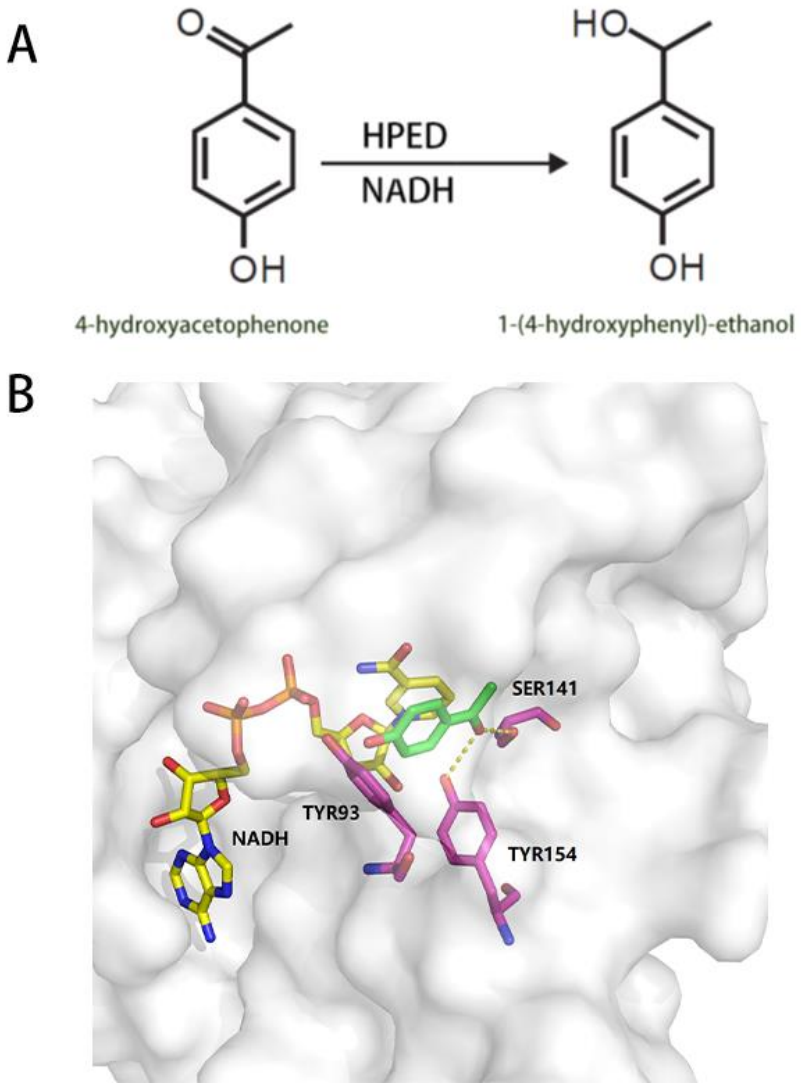

Supplementary Figure 6. (A) Reduction of 4-hydroxyacetophenone by the 1-(4-hydroxyphenyl)-ethanol dehydrogenase from strain EbN1 (HPED). (B) Functional sites involved in the formation of substrate-binding pocket of HPED (PDB ID: 2EWM) with the ligands including 4-hydroxyacetophenone and the cofactor NADH. PyMOL was used for 3D structural analysis and visualization.

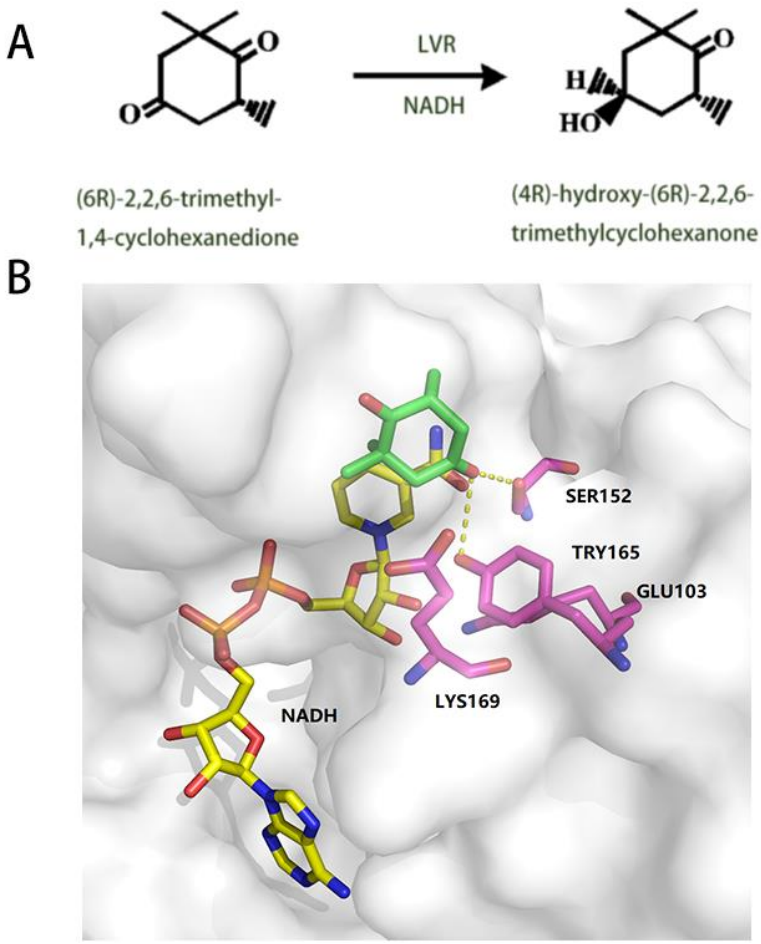

Supplementary Figure 7. (A) Conversion of (6R)-2,2,6-trimethyl-1,4-cyclohexanedione to (4R)-hydroxy-(6R)-2,2,6-trimethylcyclohexanone by levodione reductase (LVR) from *Corynebacterium aquaticum* M-13. (B) Functional sites involved in the formation of substrate-binding pocket of LVR (PDB ID: 1IY8) with the ligands including (6R)-2,2,6-trimethyl-1,4-cyclohexanedione and the cofactor NADH. PyMOL was used for 3D structural analysis and visualization.

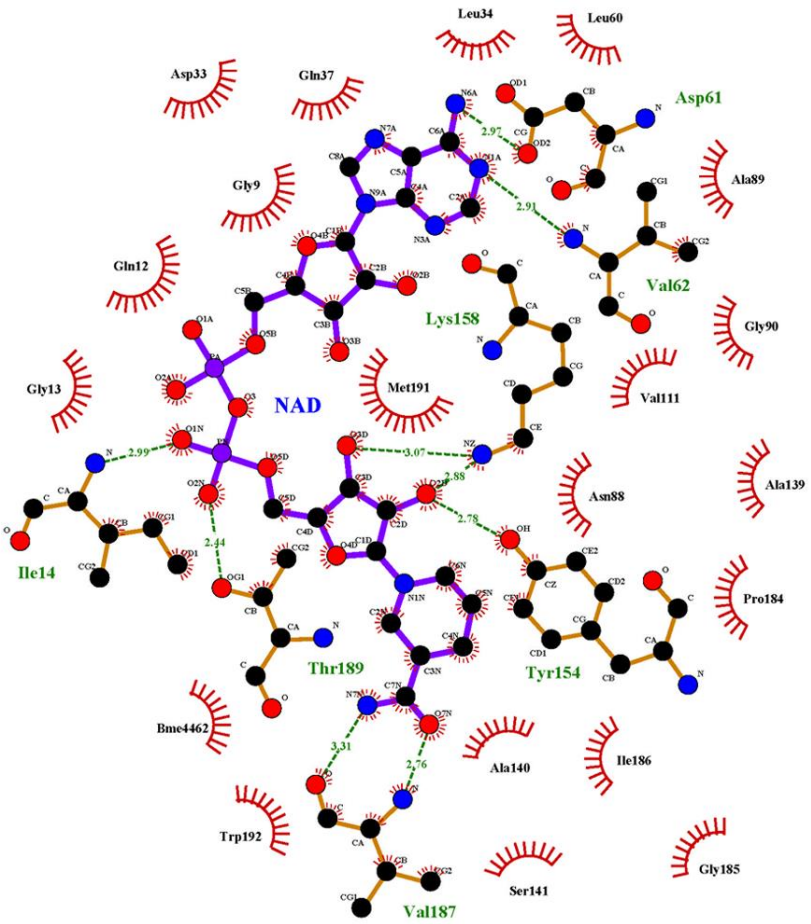

Supplementary Figure 8. Functional sites involved in cofactor binding of L-2,3-butanediol dehydrogenase (L-BDH, PDB ID: 3A28). Protein structure was retrieved from the RCSB PDB. The picture was performed with the LigPlot program.

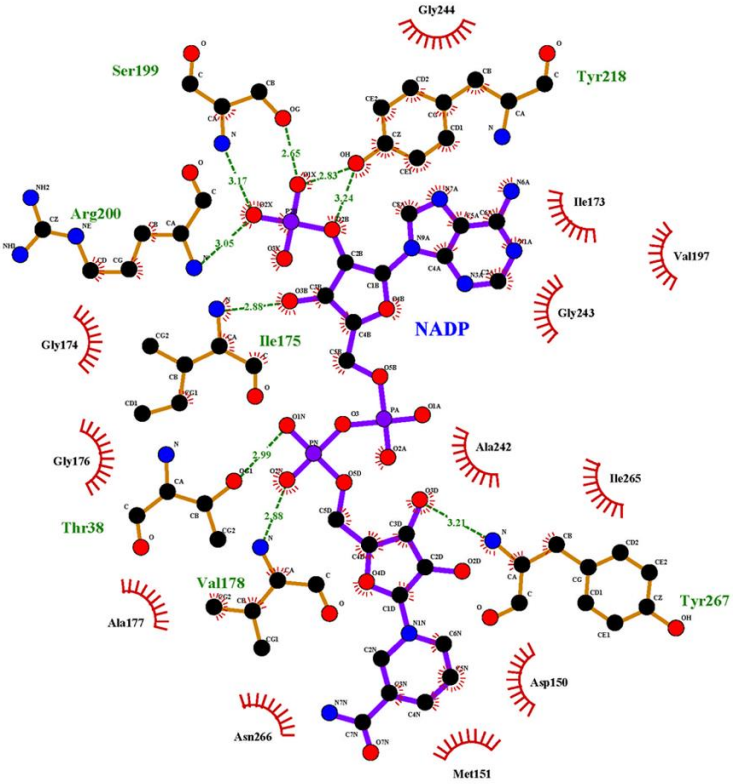

Supplementary Figure 9. Functional sites involved in cofactor binding of the alcohol dehydrogenases from *Clostridium beijerinckii* (CBADH, PDB ID: 1KEV). Protein structure was retrieved from the RCSB PDB. The picture was performed with the LigPlot program.

Supplementary Table 1 Industrial application example of asymmetric synthesis of important chiral pharmaceutical intermediates catalyzed by carbonyl reductase (3-7)

Product	Catalyst	Yield	e.e.%	Scale	Company
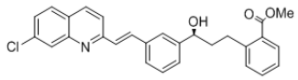	KRED	>95%	>99.9%	>200 kg	Merck
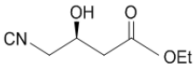	KRED/HHDH	n.d.	>99.9%	n.d.	Codexis
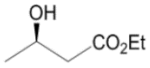	*Lactobacillus brevis* (cell extract)	96%	>99.8%	400 kg	Wacker Chemie
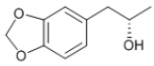	*Zygosaccharomyces rouxii*	96%	>99.9%	300 L	Eli Lilly
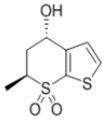	*Neurospora crassa*	>85%	>98%	Multi ton	AstraZeneca
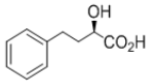	*Staphylococcus epidermidis*	91%	>99.9%	n.d.	Ciba
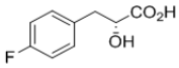	*Staphylococcus epidermidis* (isolated DHs)	99%	>99.0%	Multi kg	Pfizer
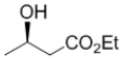	*Lactobacillus brevis* (cell extract)	96%	>99.8%	35 ta^{-1}	Wacker Chemie
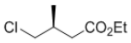	*Geotrichum candidum*	95%	>99%	Multi kg	Bristol-Myers Squibb
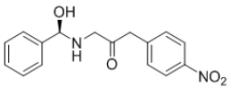	*Candida sorbophilia*	82.5%	>98%	Multi kg	Merck
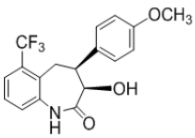	*Nocardia salmonicolor*	96%	>99.8%	n.d.	Bristol-Myers Squibb

n.d.: not disclosed.

Supplementary Table 2 Structure information of stereospecific alcohol dehydrogenases with known 3D structure

Organism	Enzyme name	PDB ID	Ligand *	Resolution (Å)	Classification	Stereo -configuration	Reference
Agrobacterium tumefaciens	Quinuclidinone reductase	3AK4	NAD	2.00	SDR	–	Not published
Bacillus subtilis	Lactate dehydrogenase	3PQD	NAD, FBP	2.38	SDR	L-specific	Not published
Brucella suis	Alcohol dehydrogenase	3MEQ	NAI, EDO, ZN	2.00	MDR	–	Not published
Candida parapsilosis	Carbonyl Reductase	3CTM (Apo)	–	2.69	SDR	Anti-prelog	8
Clostridium beijerinckii	Alcohol dehydrogenase	1PED	NDP, ZN	2.15	MDR	–	9
		1KEV		2.05			
Comamonas testosteroni	3-α-Hydroxysteroid dehydrogenase	1FJH	NAD	1.68	SDR		10
		1FK8		1.95			
Corynebacterium glutamicum	Putative short-chain dehydrogenase/reductase	3E9N (Apo)	–	2.40	SDR	–	Not published
Equus caballus	Horse liver alcohol dehydrogenase	1YE3	MPD	1.59	MDR	(4S)-MPD	11-14
		1HLD	BRB, NAD, PFB, ZN	2.10			
		1CDO	NAD, ZN	2.05			
		3BTO	NAD, SSB, ZN	1.66		(1S,3S)-SSB	
		1LDE	FPI, NAD, ZN	2.50			

		1BTO	NAD, SSB, ZN	2.00			
Escherichia coli	6-Phosphogluconate dehydrogenase	2ZYA	6PG	1.60	LDR	–	15
		2ZYD	GLO	1.50			
		3FWN	ATR	1.50			
Geobacillus stearothermophilus	Alcohol dehydrogenase	3PII	BMD	2.90	MDR	–	16
		1RJW	ETF	2.35			
Haloferax mediterranei	Glucose dehydrogenase	2B5V	NAP	2.00	MDR	–	17, 18
		2VWG	LGC, BGC, NAP, ZN	2.00			
		2VWH		2.03			
		2VWP		2.01			
		2VWQ		2.10			
Lactobacillus brevis	R-specific alcohol dehydrogenase	1NXQ,	MG	1.79	SDR	R-specific	19, 20
		1ZK4	AC0, MG, NAP	1.00			
Pseudomonas fluorescens	Mannitol dehydrogenase	1LJ8	NAD	1.70	LDR	D-specific	21
		1M2W	MTL	1.80			
Pseudomonas putida	β-D-hydroxybutyrate dehydrogenase	2Q2W		2.12	SDR	D-specific	22
		2Q2V	NAD	1.90			
		2Q2Q	NAD	2.02			
Ralstonia eutropha	2-Dehydropantoate 2-reductase	3HWR	BCN, MRD, NDP	2.15	MDR	R-specific	Not published
Rhodococcus ruber	Secondary alcohol dehydrogenase	3JV7	ACY, MPD, NAD, ZN	2.00	MDR	S-specific	23
		2XAA	BU1, NAD, ZN	2.80			
Rhodococcus sp.	L-phenylalanine dehydrogenase	1BW9	EDO, IPA, PPY, NAD	1.50	MDR	L-specific	24
		1BXG		2.30			

			HFA,IPA,PHE, NAD				25
		1C1X		1.40			
		1C1D		1.25			
Saccharomyces cerevisiae	Alcohol dehydrogenase 1	2HCY	8ID, ETF	2.44	MDR	–	Not published
Shewanella denitrificans	Iron-containing alcohol dehydrogenase	3RF7	EPE, FE, NAD, NI, PEG	2.12	MDR	–	Not published
Sphingomonas sp.	Carbonyl reductase	3AFM	NAP, TBU	1.65	SDR	–	26
		3AFN		1.63			
Sporobolomyces salmonicolor	Aldehyde reductase II	1Y1P	ACT, AMP, NMN	1.60	SDR	S-specific	27
		1ZZE		1.80			
		1UJM		2.00			
Streptococcus suis	Gluconate 5-dehydrogenase	3O03	GCO, NAP	1.90	SDR	–	28
		3CXR		2.00			
Sulfolobus solfataricus	NAD-dependent alcohol dehydrogenase	1JVB		1.85	MDR	S-specific	29-32
		1NVG		2.50			
		1NTO		1.94			
		1R37	ZN, NAD	2.30			
		3I4C	ETX	2.00			
Thermoanaerobacter brockii	NADP-dependent alcohol dehydrogenase	1YKF	NAP, ZN	2.50	MDR	–	33-36
		1BXZ	SBT, MG	2.99			
		2NVB	NAP, ZN	2.80			
		3FSR	EDO, ZN	2.20			
		3FPL	PGE, ZN	1.90			
		3FPC	ZN, EDO	1.40			
		3FTN	OXY, ACT	2.19			
Thermotoga maritima	L-lactate	1A5Z	FBP, NAD,	2.10	SDR	L-specific	37

	dehydrogenase		OXM				
Zymomonas mobilis	Alcohol	3OWO	FE2, NAD	2.07	MDR	–	Not published
	dehydrogenase 2	3OX4		2.00			

[*] 6PG, 6-phosphogluconic acid; 8ID, nicotinamide-8-iodo-adenine-dinucleotide; AC0, 1-phenylethanone; ACT, acetate ion; ACY, acetic acid; AMP, adenosine monophosphate; ATR, 2'-monophosphoadenosine-5'-diphosphate; BCN, bicine; BGC, beta-D-glucose; BMD, butyramide; BRB, para-bromobenzyl alcohol; BU1, 1,4-butanediol; EDO, 1,2-ethanediol; EPE, 4-(2-hydroxyethyl)-1-piperazine ethanesulfonic acid; ETF, trifluoroethanol; ETX, 2-ethoxyethanol; FBP, beta-fructose-1,6-diphosphate; FE, Fe (iii) ion; FPI, n-formylpiperidine; GCO, gluconic acid; GLO, D-glucose in linear form; HFA, alpha-hydroxy-beta-phenyl-propionic acid; IPA, isopropyl alcohol; LGC, (3s,4r,5r,6s)-3,4,5-trihydroxy-6-(hydroxymethyl)tetrahydro-2h-pyran-2-one; MG, magnesium ion; MPD, (4s)-2-methyl-2,4-pentanediol; MRD, (4r)-2-methylpentane-2,4-diol; NAD, nicotinamide-adenine-dinucleotide; NAP, NADP nicotinamide-adenine-dinucleotide phosphate; NDP, NADPH dihydro-nicotinamide-adenine-dinucleotide phosphate; NI, nickel (ii) ion; NMN, beta-nicotinamide ribose monophosphate; OXM, oxamic acid; OXY, oxygen molecule; PEG, di(hydroxyethyl) ether; PFB, 2,3,4,5,6-pentafluorobenzyl alcohol; PHE, phenylalanine; PPY, 3-phenylpyruvic acid; SBT, 2-butanol; SSB, 3-butylthiolane 1-oxide; TBU, tertiary-butyl alcohol; ZN, zinc ion.

Supplementary Table 3 Properties of various stereospecific alcohol dehydrogenases*

Microorganism	Enzyme	Mr (kDa)	Oligomer	Cofactor	Optimum pH/T (ºC)	Substrate	Product config.	Reference
Ancylobacter aquaticus	FDH	90	Dimer	NAD^+	6.3/50	Aldehydes/carboxylic acids	—	38
Candida macedoniensis	MR	45	Monomer	NADPH	6.5/40	COBE	S	39, 40
Candida magnoliae	R	33	Monomer	NADPH	7.0/40	COBE/ketoesters/aldehydes	R	41, 42
	S1	77	Dimer		5.5/55		S	
	S4	86	Trimer		6.0/50		S	
Candida parapsilosis	RCR	35	Monomer	NADH	6.0/45	Secondary alcohols/ketones	R	43
Candida parapsilosis	CPADH	30	Monomer	NADPH	4.5/35	Ketones	S	44
Candida parapsilosis	SADH	140	Tetramer	NAD^+	6.0/—	BDO/secondary alcohols	R	45
Candida parapsilosis	C1	38	Monomer	NADPH	7.5/50	ketopantoyl lactone,	D	46, 47
	C2	36	Monomer		7.0/40	conjugated polyketone		
Corynebacterium sp.	PAR	155	Tetramer	NADH	6.0-6.5/—	2-alkanones, aromatic ketones	S	48
Lactobacillus kefir	ADH	—	—	NADPH	7.0/—	Acetophenone, ketones	R	49
Nocardia fusca	ADH	150	Tetramer	NAD^+	5.5-6.5/65	PTO/secondary alcohols	R	50
Penicillium citrinum	AKR	37	Monomer	NADPH	6.5/—	Aldehydes/ ketones	S	51
Pseudomonas fluorescens	ADH	32	Monomer	NADH	8.0/20	Alcohols	R	52
Rhodococcus erythropolis	ALDH	162	Trimer	NAD^+	9.5-10/47	Aldehydes	—	53
Rhodotorula glutinis	CR	40	Monomer	NADPH	5-6/40-50	Ketones	R	54
Sporobolomyces salmonicolor	AR Ⅰ	37	Monomer	NADPH	7.0/60	COBE, aldehyde, ketoesters	R	55;
	AR Ⅱ	34	Monomer		5.5/40		S	56, 57
	AR Ⅲ	37	Monomer		—/—		R	
Thiobacillus sp.	FDH	90	Dimer	NAD^+	5.6/58	Aldehydes/carboxylic acids	—	58

Zygosaccharomyces rouxii	KR	42	Monomer	NADPH	6.6-6.8/37-39	MDA	S	59

[*a] FDH: formate dehydrogenase; MR, Menadione reductase; AR, aldehyde reductase; RCR, (*R*)-specific carbonyl reductases; CPADH, *Candida parapsilosis* alcohol dehydrogenase; SADH, secondary alcohol dehydrogenase; C1, conjugated polyketone reductase 1; C2, conjugated polyketone reductase 2; PAR, phenylacetaldehyde reductase; ADH: alcohol dehydrogenase; AKR: aldo-keto reductase; ALDH: aldehyde dehydrogenase; KR, ketone reductase; COBE: ethyl 4-chloro-3-oxobutyrate, MOB, Methyl 3-oxobutanoate; BDO, 1,3-butanediol; PTO, 3-pentyn-2-ol; MDA, 3,4-methylene-dioxyphenyl acetone.

Supplementary Table 4 Organic solvent tolerance and thermostable ADHs

Enzyme	Source	Cofactor	Additional information	Reference
TBADH	*Thermoanaerobacter brockii*	NADP(H)	TBADH reversibly catalyzes the oxidation of secondary alcohols to the corresponding ketones. It exhibited good retention of activity in organic solvents: acetone was tolerated at up to 50% concentration and in two-phase systems with hexane and octane, up to 80% activity was conserved. he half the activity is lost after 1 h of incubation is 93°C, and the melting temperature is 98°C	60, 61
CBADH	*Clostridium beijerinckii*	NADP(H)	It is thermostable (half-life of 1 h at 63.8°C). It can reduce acetoin to (R,R)- 2,3-butanediol (92 g/L, ee 90%, 56 h).	62
TeSADH	*Thermoanaerobacter ethanolicus*	NADP+	The wild-type enzyme is in general (S)-selective (except 2-butanone) and not active towards any aromatic compounds or more sterically demanding substrates. It retains 90%, 100%, 80% and 68% activity after a 3-h incubation in 100% n-dodecane, n-octane, toluene and pyridine, respectively. It is optimally active near 90°C, thermostable (half-life of 1.7 h at 90°C)	63, 64
TKADH	*Thermococcus kodakarensis* KOD1	NAD^+	The substrates are secondary alcohols and accepted various ketones and aldehydes. For example, TkADH could also reduce 2,2,2-trifluoroacetophenone to (*R*)-2,2,2-trifluoro-1-phenylethanol with high enantioselectivity (>99.6% ee). he enzyme showed high resistance to organic solvents and was particularly highly active in the presence of H2O–20% 2-propanol and H2O–50% *n*-hexane or *n*-octane. It was highly thermostable with an optimal temperature of 90°C and a half-life of 4.5 h at 95°C.	65
ADH-‘A’	*Rhodococcus ruber*	NADH		66, 67

			It was applied to ketone–alcohol conversions in both the oxidative and reductive directions high tolerance toward organic solvents, particularly acetone (up to 50%, v/v), 2-propanol (up to 80%, v/v), and hexane (up to 99%, v/v)	
PFADH	*Pyrococcus furiosus*	NADH		68
			It catalyzes the reduction of various ketones including aryl ketones, a- and b-ketoesters usually display not only an extreme stability at a high temperature (a half-life of 130 min at 100 °C) and high pressure, but also a high tolerance of chemical denaturants such as organic solvent	
Pcal_1311	*Pyrobaculum calidifontis*	NAD^+		69
			Pcal_1311 catalyzed the NAD(H)-dependent oxidation of various alcohols and reduction of aldehydes, with a marked preference for substrates with functional group at the terminal carbon. Pcal_1311 was highly stable and retained more than 90% activity even after incubation of 180 min at 90 °C	
HvADH2	*Haloferax volcanii*	NAD^+		69,
			showed an unusually broad substrate specificity, with good activity with medium-chain alcohols, modest activity with secondary alcohols and also significant activity with benzyl alcohol . The HvADH2 showed remarkable stability and catalysed the reaction in aqueous–organic medium containing dimethyl sulfoxide (DMSO) and methanol (MeOH).	
ChnA	*Azoarcus* sp. EbNl	$NAD(P)^+$		70
Ebn2	*Azoarcus* sp. EbNl	$NAD(P)^+$	The alcohol dehydrogenases ChnA and Ebn2 accept various simple alcohols as reducing agents. They are oxidized to the corresponding carbonyl compounds. Simple alcohols which are suitable for regenerating NADH or NADPH are iso-propanol, butan-2-ol and pentan-2-ol.	

References

1. Robert X, Gouet P. Deciphering key features in protein structures with the new ENDscript server. Nucleic Acids Res. 2014;42:W320-4.
2. Katoh K, Rozewicki J, Yamada KD. MAFFT online service: multiple sequence alignment, interactive sequence choice and visualization. Brief Bioinform. 2017 Sep 6.
3. Thayer A M. Biocatalysis helps reach a resolution. Chemical & Engineering News, 2006;84:29-31.
4. Liang J, Lalonde J, Borup B. Development of a biocatalytic process as an alternative to the (−)-DIP-Cl-mediated asymmetric reduction of a key intermediate of montelukast. Organic Process Research & Development, 2009;14:193-198.
5. Fox R J, Davis S C, Mundorff E C. Improving catalytic function by ProSAR-driven enzyme evolution[J]. Nature Biotechnology, 2007;25:338-344.
6. Tao J, Xu J-H. Biocatalysis in development of green pharmaceutical processes. Current Opinion in Chemical Biology, 2009;3:43-50.
7. Liese A, Seelbach K, Wandrey C. Industrial biotransformations. John Wiley & Sons, 2006.
8. Zhang R, Zhu G, Zhang W, Cao S, Ou X, Li X, Bartlam M, Xu Y, Zhang XC, Rao Z. Crystal structure of a carbonyl reductase from *Candida parapsilosis* with anti-prelog stereospecificity. Protein Sci, 2008;17:1412-23.
9. Korkhin Y, Frolow F, Bogin O, Peretz M, Kalb AJ, Burstein Y. Crystalline alcohol dehydrogenases from the mesophilic bacterium *Clostridium beijerinckii* and the thermophilic bacterium *Thermoanaerobium brockii*: preparation, characterization and molecular symmetry. Acta Cryst D, 1996;52:882-6.
10. Grimm C, Maser E, Mobus E, Klebe G, Reuter K, Ficner R. The crystal structure of 3α-hydroxysteroid dehydrogenase/carbonyl reductase from *Comamonas testosteroni* shows a novel oligomerization pattern within the short chain dehydrogenase/reductase family. J Biol Chem, 2000;275:41333-9.
11. Ramaswamy S, Eklund H, Plapp BV. Structures of horse liver alcohol dehydrogenase complexed with NAD^+ and substituted benzyl alcohols. Biochemistry, 1994;33:5230-7.
12. Ramaswamy S, Ahmad ME, Danielsson O, Jörnvall H, Eklund H. Crystal structure of cod liver class I alcohol dehydrogenase: substrate pocket and structurally variable segments. Protein Sci, 1996;5:663-71.
13. Cho H, Ramaswamy S, Plapp BV. Flexibility of liver alcohol dehydrogenase in stereoselective binding of 3-butylthiolane 1-oxides. Biochemistry, 1997;36:382-9.
14. Ramaswamy S, Scholze M, Plapp BV. Binding of formamides to liver alcohol dehydrogenase. Biochemistry, 1997;36:3522-7.
15. Chen Y-Y, Ko T-P, Chen W-H, Lo L-P, Lin C-H, Wang AHJ. Conformational changes associated with cofactor/substrate binding of

6-phosphogluconate dehydrogenase from *Escherichia coli* and *Klebsiella pneumoniae*: implications for enzyme mechanism. J Struct Biol, 2010;169:25-35.
16. Ceccarelli C, Liang Z-X, Strickler M, Prehna G, Goldstein BM, Klinman JP, Bahnson BJ. Crystal structure and amide H/D exchange of binary complexes of alcohol dehydrogenase from *Bacillus stearothermophilus*: insight into thermostability and cofactor binding. Biochemistry, 2004;43:5266-77.
17. Britton KL, Baker PJ, Fisher M, Ruzheinikov S, Gilmour DJ, Bonete MJ, Ferrer J, Pire C, Esclapez J, Rice DW. Analysis of protein solvent interactions in glucose dehydrogenase from the extreme halophile *Haloferax mediterranei*. Proc Natl Acad Sci U S A, 2006;103:4846-51.
18. Baker PJ, Britton KL, Fisher M, Esclapez J, Pire C, Bonete MJ, Ferrer J, Rice DW. Active site dynamics in the zinc-dependent medium chain alcohol dehydrogenase superfamily. Proc Natl Acad Sci U S A, 2009;106:779-84.
19. Niefind K, Müller J, Riebel B, Hummel W, Schomburg D. The crystal structure of *R*-specific alcohol dehydrogenase from *Lactobacillus brevis* suggests the structural basis of its metal dependency. J Mol Biol, 2003;327:317-28.
20. Schlieben NH, Niefind K, Müller J, Riebel B, Hummel W, Schomburg D. Atomic resolution structures of *R*-specific alcohol dehydrogenase from *Lactobacillus brevis* provide the structural bases of its substrate and cosubstrate specificity. J Mol Biol, 2005;349:801-13.
21. Kavanagh KL, Klimacek M, Nidetzky B, Wilson DK. Crystal structure of *Pseudomonas fluorescens* mannitol 2-dehydrogenase binary and ternary complexes. Specificity and catalytic mechanism. J Biol Chem, 2002;277:43433-42.
22. Paithankar KS, Feller C, Kuettner EB, Keim A, Grunow M, Sträter N. Cosubstrate-induced dynamics of D-3-hydroxybutyrate dehydrogenase from *Pseudomonas putida*. FEBS J, 2007;274:5767-79.
23. Karabec M, Łyskowski A, Tauber KC, Steinkellner G, Kroutil W, Grogan G, Gruber K. Structural insights into substrate specificity and solvent tolerance in alcohol dehydrogenase ADH-‘A’ from *Rhodococcus ruber* DSM 44541. Chem Commun, 2010;46:6314-6.
24. Vanhooke JL, Thoden JB, Brunhuber NMW, Blanchard JS, Holden HM. Phenylalanine dehydrogenase from *Rhodococcus* sp. M4: high-resolution X-ray analyses of inhibitory ternary complexes reveal key features in the oxidative deamination mechanism. Biochemistry, 1999;38;2326-39.
25. Brunhuber NMW, Thoden JB, Blanchard JS, Vanhooke JL. *Rhodococcus* L -phenylalanine dehydrogenase: kinetics, mechanism, and structural basis for catalytic specifity. Biochemistry, 2000;39:9174-87.
26. Takase R, Ochiai A, Mikami B, Hashimoto W, Murata K. Molecular identification of unsaturated uronate reductase prerequisite for alginate metabolism in *Sphingomonas* sp. A1. Biochem Biophys Acta, 2010;1804:1925-36.
27. Kamitori S, Iguchi A, Ohtaki A, Yamada M, Kita K. X-ray structures of NADPH-dependent carbonyl reductase from *Sporobolomyces salmonicolor* provide insights into stereoselective reductions of carbonyl compounds. J Mol Biol, 2005;352:551-8.

28. Zhang Q, Peng H, Gao F, Liu Y, Cheng H, Thompson J, Gao GF. Structural insight into the catalytic mechanism of gluconate 5-dehydrogenase from *Streptococcus suis*: crystal structures of the substrate-free and quaternary complex enzymes. Protein Sci, 2009;18:294-303.
29. Esposito L, Bruno I, Sica F, Raia CA, Giordano A, Rossi M, Mazzarella L, Zagari A. Crystal structure of a ternary complex of the alcohol dehydrogenase from *Sulfolobus solfataricus*. Biochemistry, 2003a;42:14397-407.
30. Esposito L, Bruno I, Sica F, Raia CA, Giordano A, Rossi M, Mazzarella L, Zagari A. Structural study of a single-point mutant of *Sulfolobus solfataricus* alcohol dehydrogenase with enhanced activity. FEBS Lett, 2003b:539:14-8.
31. Esposito L, Sica F, Raia CA, Giordano A, Rossi M, Mazzarella L, Zagari A. Crystal Structure of the alcohol dehydrogenase from the hyperthermophilic archaeon *Sulfolobus solfataricus* at 1.85Å resolution. J Mol Biol, 2002;318:463-77.
32. Pennacchio A, Esposito L, Zagari A, Rossi M, Raia CA. Role of Tryptophan 95 in substrate specificity and structural stability of *Sulfolobus solfataricus* alcohol dehydrogenase. Extremophiles, 2009;13:751-61.
33. Korkhin Y, Kalb AJ, Peretz M, Bogin O, Burstein Y, Frolow F. NADP-dependent bacterial alcohol dehydrogenases: crystal structure, cofactor-binding and cofactor specificity of the ADHs of *Clostridium beijerinckii* and *Thermoanaerobacter brockii*. J Mol Biol, 1998;278:967-81
34. Li C, Heatwole J, Soelaiman S, Shoham M. Crystal structure of a thermophilic alcohol dehydrogenase substrate complex suggests determinants of substrate specificity and thermostability. Proteins, 1999;37:619-27.
35. Goihberg E, Dym O, Tel-Or S, Shimon L, Frolow F, Peretz M, Burstein Y. Thermal stabilization of the protozoan *Entamoeba histolytica* alcohol dehydrogenase by a single proline substitution. Proteins, 2008;72:711-9.
36. Goihberg E, Peretz M, Tel-Or S, Dym O, Shimon L, Frolow F, Burstein Y. Biochemical and structural properties of chimeras constructed by exchange of cofactor-binding domains in alcohol dehydrogenases from thermophilic and mesophilic microorganisms. Biochemistry, 2010;49:1943-53.
37. Auerbach G, Ostendorp R, Prade L, Korndörfer I, Dams T, Huber R, Jaenicke R. Lactate dehydrogenase from the hyperthermophilic bacterium thermotoga maritima: the crystal structure at 2.1 A resolution reveals strategies for intrinsic protein stabilization. Structure, 1998;6:769-81.
38. Nanba H, Takaoka Y, Hasegawa J. Purification and characterization of formate dehydrogenase from *Ancylobacter aquaticus* strain KNK607M, and cloning of the gene. Biosci Biotechnol Biochem, 2003b;67:720-8.
39. Kataoka M, Hoshino-Hasegawa A, Thiwthong R, Higuchi N, Ishige T, Shimizu S. Gene cloning of an NADPH-dependent menadione reductase from *Candida macedoniensis*, and its application to chiral alcohol production. Enzyme Microb Technol, 2006;38:944-51.

40. Kataoka M, Kotaka A, Thiwthong R, Wada M, Nakamori S, Shimizu S. Cloning and overexpression of the old yellow enzyme gene of *Candida macedoniensis*, and its application to the production of a chiral compound. J Biotechnol, 2004b;114:1-9.
41. Wada M, Kataoka M, Kawabata H, Yasohara Y, Kizaki N, Hasegawa J, Shimizu S. Purification and characterization of NADPH-dependent carbonyl reductase, involved in stereoselective reduction of ethyl 4-chloro-3-oxobutanoate, from *Candida magnoliae*. Biosci Biotechnol Biochem, 1998;62:280-5.
42. Wada M, Kawabata H, Yoshizumi A, Kataoka M, Nakamori S, Yasohara Y, Kizaki N, Hasegawa J, Shimizu S. Occurrence of multiple ethyl 4-chloro-3-oxobutanoate-reducing enzymes in *Candida magnoliae*. J Biosci Bioeng, 1999;87:144-8.
43. Nie Y, Xu Y, Yang M, Mu XQ. A novel NADH-dependent carbonyl reductase with unusual stereoselectivity for (*R*)-specific reduction from an (*S*)-1-phenyl-1,2-ethanediol-producing micro-organism: purification and characterization. Lett Appl Microbiol, 2007b;44:555-62.
44. Nie Y, Xu Y, Mu XQ, Wang HY, Yang M, Xiao R. Purification, characterization, gene cloning, and expression of a novel alcohol dehydrogenase with anti-prelog stereospecificity from *Candida parapsilosis*. Appl Environ Microbiol, 2007a;73:3759-64.
45. Yamamoto H, Kawada N, Matsuyama A, Kobayashi Y. Cloning and expression in *Escherichia coli* of a gene coding for a secondary alcohol dehydrogenase from *Candida parapsilosis*. Biosci Biotechnol Biochem, 1999;63:1051-5.

46. Hidalgo A-RGD, Akond MA, Kita K, Kataoka M, Shimizu S. Isolation and primary structural analysis of two conjugated polyketone reductases from *Candida parapsilosis*. Biosci Biotechnol Biochem, 2001;65:2785-8.
47. Kataoka M, Delacruz-Hidalgo ARG, Akond MA, Sakuradani E, Kita K, Shimizu S. Gene cloning and overexpression of two conjugated polyketone reductases, novel aldo-keto reductase family enzymes, of *Candida parapsilosis*. Appl Microbiol Biotechnol, 2004a;64:359-66.
48. Itoh N, Morihama R, Wang J, Okada K, Mizuguchi N. Purification and characterization of phenylacetaldehyde reductase from a styrene-assimilating *Corynebacterium* strain, ST-10. Appl Environ Microbiol, 1997;63:3783-8.
49. Bradshaw CW, Hummel W, Wong CH. *Lactobacillus kefir* alcohol dehydrogenase: a useful catalyst for synthesis. J Org Chem, 1992;57:1532-6.
50. Xie S-X, Ogawa J, Shimizu S. NAD^+-Dependent (*S*)-specific secondary alcohol dehydrogenase involved in stereoinversion of 3-pentyn-2-ol catalyzed by *Nocardia fusca* AKU 2123. Biosci Biotechnol Biochem, 1999;63:1721-9.
51. Itoh N, Asako H, Banno K, Makino Y, Shinohara M, Dairi T, Wakita R, Shimizu M. Purification and characterization of NADPH-dependent aldo-keto reductase specific for β-keto esters from *Penicillium citrinum*, and production of methyl (*S*)-4-bromo-3-hydroxybutyrate. Appl Microbiol Biotechnol, 2004;66:53-62.
52. Hildebrandt P, Musidlowska A, Bornscheuer UT, Altenbuchner J. Cloning, functional expression and biochemical characterization of a stereoselective alcohol dehydrogenase from *Pseudomonas fluorescens* DSM50106. Appl Microbiol Biotechnol, 2002;59:483-7.
53. Jaureguibeitia A, Saá L, Llama MJ, Serra JL. Purification, characterization and cloning of aldehyde dehydrogenase from *Rhodococcus erythropolis* UPV-1. Appl Microbiol Biotechnol, 2006;73:1073-86.
54. Kizaki N, Sawa I, Yano M, Yasohara Y, Hasegawa J. Purification and Characterization of a yeast carbonyl reductase for synthesis of optically active (*R*)-Styrene oxide derivatives. Biosci Biotechnol Biochem, 2005;69:79-86.
55. Kataoka M, Sakai H, Morikawa T-I, Katoh M, Miyoshi T, Shimizu S, Yamada H. Characterization of aldehyde reductase of *Sporobolomyces salmonicolor*. Biochim Biophys Acta, 1992;1122:57-62.
56. Kita K, Matsuzaki K, Hashimoto T, Yanase H, Kato N, Chung MC, Kataoka M, Shimizu S. Cloning of the aldehyde reductase gene from a red yeast, *Sporobolomyces salmonicolor*, and characterization of the gene and its product. Appl Environ Microbiol, 1996;62:2303-10.
57. Kita K, Nakase K-I, Yanase H, Kataoka M, Shimizu S. Purification and characterization of new aldehyde reductases from *Sporobolomyces salmonicolor* AKU4429. J Mol Catal B Enzym, 1999;6:305-13.
58. Nanba H, Takaoka Y, Hasegawa J. Purification and characterization of an α-haloketone-resistant formate dehydrogenase from *Thiobacillus* sp. strain KNK65MA, and Cloning of the gene. Biosci Biotechnol Biochem, 2003a;67:2145-53.
59. Costello CA, Payson RA, Menke MA, Larson JL, Brown KA, Tanner JE, Kaiser RE, Hershberger CL, Zmijewski MJ. Purification, characterization, cDNA cloning and expression of a novel ketoreductase from *Zygosaccharomyces rouxii*. Eur J Biochem,

2000;267;5493-501.
60. Li C, Heatwole J, Soelaiman S, Shoham M. Crystal structure of a thermophilic alcohol dehydrogenase substrate complex suggests determinants of substrate specificity and thermostability. Proteins: Structure, Function and Genetics, 1999;37: 619-627.
61. Morra S， Pordea A. Biocatalyst – artificial metalloenzyme cascade based on alcohol dehydrogenase. Chem Sci, 2018;9:7447–7454.
62. Bogin O, Peretz M, Hacham Y, Korkhin Y, Frolow F, Kalb(Gilboa) AJ, Burstein Y. Enhanced thermal stability of Clostridium beijerinckii alcohol dehydrogenase after strategic substitution of amino acid residues with prolines from the homologous thermophilic Thermoanaerobacter brockii alcohol dehydrogenase. Protein Sci. 1998,May;7:1156-63.
63. Ziegelmann-Fjeld KI, Musa MM, Phillips RS, Zeikus JG, Vieille C. A Thermoanaerobacter ethanolicus secondary alcohol dehydrogenase mutant derivative highly active and stereoselective on phenylacetone and benzylacetone. Protein Eng Des Sel;2007;20:47-55.
64. Popłoński J, Reiter T, Kroutil W. Biocatalytic Racemization Employing TeSADH: Substrate Scope and Organic Solvent Compatibility for Dynamic Kinetic Resolution. ChemCatChem 2018;10:763-768.
65. Wu X, Zhang C, Orita I, Imanaka T, Fukui T, Xing XH. Thermostable alcohol dehydrogenase from Thermococcus kodakarensis KOD1 for enantioselective bioconversion of aromatic secondary alcohols. Appl Environ Microbiol. 2013;79:2209-17.
66. Höfler GT, Fernández-Fueyo E, Pesic M, Younes S, Choi EG, Kim YH, Urlacher V, Arends I, Hollmann F. A photoenzymatic NADH regeneration system. Chembiochem. 2018 10. 1002/cbic.201800530.
67. Karabec M, Łyskowski A, Tauber KC, Steinkellner G, Kroutil W, Grogan G, Gruber K. Structural insights into substrate specificity and solvent tolerance in alcohol dehydrogenase ADH-‘A’ from Rhodococcus ruber DSM 44541. Chem Commun, 2010;46:6314-6.
68. Ashraf R, Rashid N, Kanai T, Imanaka T, Akhtar M. Pcal_1311, an alcohol dehydrogenase homologue from Pyrobaculum calidifontis, displays NADH-dependent high aldehyde reductase activity. Extremophiles. 2017;21:1101-1110.
69. Cassidy J, Bruen L, Rosini E, Molla G, Pollegioni L, Paradisi F. Engineering substrate promiscuity in halophilic alcohol dehydrogenase (HvADH2) by in silico design. PLoS One. 2017;12:e0187482.
70. Michael Breuer D; Ralf Rabus B; Johann Heider M. Method for producing optically active alcohols using an azoarcus sp. Ebn1 dehydrogenase. 2012;Patent US 8338146B2.

1